Measurement of the Inclusive Semi-muonic Decay Branching Fractions of $D^+(D^0)$ Mesons at $\sqrt{s}$=4.03GeV

Xu Chuncheng Yan Wuguang RongGang
Institute of High Energy Physics
Chinese Academy of Sciences
Beijing, China

February 26, 1997

Abstract

In this MEMO the determination of inclusive semi-muonic decay branching fractions of $D^+(D^0) \to \mu^+ X$ is reported. We have selected D candidate events by reconstructing four hadronic decay modes $D^0 \to K^-\pi^+$, $D^0 \to K^-\pi^+\pi^+\pi^-$, $D \to K^-\pi^+\pi^+$ and $D \to K^0\pi^+$ coming from reactions $e^+e^- \to \psi(4030) \to DD^*, D^*D^*$ and have searched for inclusive μ(both right sign and wrong sign) in the recoiling side against tagged neutral and charged D mesons. We observed 5872 ± 260 singly tagged D^0 events and 2068 ± 161 singly tagged D^+ events. We got 90.02 ± 10.13 and 39.91 ± 6.31 "net" right sign muons in the recoiling side against D^0 and D^+ single tags separately. This leads to the branching fractions $B(D^+ \to \mu^+ X) = (17.28 \pm 6.13 \pm 2.14)\%$ and $B(D^0 \to \mu^+ X) = (8.12 \pm 2.09 \pm 0.69)\%$.

1 Introduction

Measurement of the values of the inclusive semi-muonic decay branching fractions of the charged and neutral D mesons is very significant both experimentally and theoretically. The decay branching fractions can help us understand the weak decay properties of D measons in some way. According to the theory of the universality of weak interaction, the inclusive μ decay branching fractions of D^+ and D^0 should be very close to those of inclusive e which are available in PDG. They can also be used to check the exclusive μ decay branching fractions of D^+ and D^0. PDG94 gives $B(D^0 \to \mu^+ X) = (10.0^{+2.6}_{-2.6})\%$. PDG96 gives $B(D^0 \to \mu^+ X) = (6.8^{+1.0}_{-1.0})\%$. The inclusive decay branching fraction of $D^+ \to \mu^+ X$ is not available in particle booklet. We would give the result of the inclusive semi-muonic decay branching fraction for first measurement.

Before further discussion, here in the paper we define one μ^- track against a D^+ or D^0 single tag (or μ^+ track against a D^- or $\bar{D}^0$ single tag) a so called 'right sign" muon. We also define one μ^- track against a D^- or $\bar{D}^0$ single tag (or μ^+ track against a D^+ or D^0 single tag) a so called 'wrong sign" muon. All the process of D decay described below reprents the process itself and its charge conjugate process combined.

In the following we will first try to find the numbers of candidate e, μ, π and K in the recoiling side against the tagged neutral and charged D measons. Then we will unfold these numbers into the numbers of real e, μ, π and K by using the particle identification effiencies and misidentification rates which are got from using data sample of e, μ, π and K. We will also use Monto Carlo data to study the general effiency of finding μ in the recoiling side against the tagged neutral and charged D measons. Finally we will give out the inclusive semi-muonic branching fractions of the charged and neutral D mesons and do their error analysis.

2 The "Method of Combining D^+ and D^0 tags together"

At $\sqrt{s} = 4.03GeV$ the charm mesons are produced in process

$$e^+e^- \to \psi(4030) \to D_s^+D_s^-, D^+D^-, D^0\bar{D}^0$$

$\rightarrow D^{\pm} D^{*\mp}$
$\rightarrow D^0 \bar{D}^{*0} (\bar{D}^0 D^{*0})$
$\rightarrow D^{*\pm} D^{*\mp}$
$\rightarrow D^{*0} \bar{D}^{*0}$

where the $D^{*\pm} \rightarrow \gamma D^{\pm}$ $(BF = 1.11\%$ $PDG)$
$\rightarrow \pi^0 D^{\pm}$ $(BF = 30.8\%$ $PDG)$
$\rightarrow \pi^{\pm} D^0$ $(BF = 68.1\%$ $PDG)$
and $D^{*0} \rightarrow \gamma D^0$ $(BF = 36.4\%$ $PDG)$
$\rightarrow \pi^0 D^0$ $(BF = 63.6\%$ $PDG)$

Most of the productions are $D^+ D^{*-}$ (or $D^{*+} D^{*-}$) and $D^0 \bar{D}^{*0}$ (or$D^{*0} \bar{D}^{*0}$). We can not tell whether a $\bar{D}^0$ or D^- have occurred in the recoiling side against a D^0 or D^+ single tag due to the D^{*+} decay channel of $D^{*+} \rightarrow \pi^+ D^0$. However, we can know the probabilities of D^-'s occurrance and $\bar{D}^0$'s occurrance against the D^+ (or D^0) single tag, provided that the cross sections of $D^+ D^{*-}$ (or $D^{*+} D^{*-}$) and $D^0 \bar{D}^{*0}$(or$D^{*0} \bar{D}^{*0}$) and $Br(D^{*+} \rightarrow \pi^+ D^0)$ are known. The proportion of D^-'s occurrance to $\bar{D}^0$'s occurrance against a D^+ single tag leads to a certain number of particle P that occurred against per D^+ single tag, while the proportion of D^-'s occurrance to $\bar{D}^0$'s occurrance against a D^0 single tag leads to another number of particle P that occurred against per D^0 single tag. So the particle P inclusive branching fractions of D^+ and D^0 can easily be solved out. This is called the **"Method of Combining D^+ and D^0 tags together ".**[1]

Suppose we want to measure a particle P inclusive decay branching fractions of the D^+ and D^0, we should search for the particle P and count the numbers ($N^P_{D^+_{tag}}$ and $N^P_{D^0_{tag}}$) of the particle P appeared in the recoiling side against the tagged D^+ and D^0, respectively. This is called 'Double-Tags' in the paper. The $N^P_{D^0_{tag}}$ is related to $N^{D^-}_{D^0_{tag}}$ and $N^{\bar{D}^0}_{D^0_{tag}}$ which respectively are numbers of D^- and $\bar{D}^0$ produced in the recoiling system against to the tagged D^0 sample by

$$N^P_{D^0_{tag}} = \epsilon_1 \times N^{D^-}_{D^0_{tag}} \times BF(D^- \rightarrow P\ X) + \epsilon_2 \times N^{\bar{D}^0}_{D^0_{tag}} \times BF(\bar{D}^0 \rightarrow P\ X), \tag{1}$$

where ϵ_1 and ϵ_2 are efficiencies for detection of the particle P, $BF(D^- \rightarrow P\ X)$ and $BF(\bar{D}^0 \rightarrow PX)$ are decay branching fractions to be extracted. Similarly, for D^+ tags we have

$$N^P_{D^+_{tag}} = \epsilon'_1 \times N^{D^-}_{D^+_{tag}} \times BF(D^- \rightarrow P\ X) + \epsilon'_2 \times N^{\bar{D}^0}_{D^+_{tag}} \times BF(\bar{D}^0 \rightarrow P\ X) \tag{2}$$

where ϵ'_1 and ϵ'_2 are also efficiencies. By combining the (1) and (2) together, we can extract the inclusive decay branching fractions of D^- and $\bar{D}^0$ as following

$$BF(D^- \rightarrow P\ X) = \frac{N^{\bar{D}^0}_{D^0_{tag}} \times N^P_{D^+_{tag}} - N^{\bar{D}^0}_{D^+_{tag}} \times N^P_{D^0_{tag}}}{\epsilon \times (N^{\bar{D}^0}_{D^0_{tag}} \times N^{D^-}_{D^+_{tag}} - N^{\bar{D}^0}_{D^+_{tag}} \times N^{D^-}_{D^0_{tag}})}, \tag{3}$$

$$BF(\bar{D}^0 \rightarrow P\ X) = \frac{N^{D^-}_{D^+_{tag}} \times N^P_{D^0_{tag}} - N^{D^-}_{D^0_{tag}} \times N^P_{D^+_{tag}}}{\epsilon \times (N^{D^-}_{D^+_{tag}} \times N^{\bar{D}^0}_{D^0_{tag}} - N^{D^-}_{D^0_{tag}} \times N^{\bar{D}^0}_{D^+_{tag}})}. \tag{4}$$

Where $N^{\bar{D}^0}_{D^+_{tag}}$ is the number of $\bar{D}^0$ produced in the recoiling system against the tagged D^+, $N^{D^-}_{D^+_{tag}}$ is the number of D^- produced in the recoiling system against the tagged D^+ and ϵ ($\epsilon \approx \epsilon_1 \approx \epsilon_2 \approx \epsilon'_1 \approx \epsilon'_2$) is the efficiency for detection of the particle P. Using the numbers ($N_{D^0_{tag}}$ and $N_{D^+_{tag}}$) of the D^0 and D^+ single tags, we can calculate the numbers of the $\bar{D}^0$ and D^- produced in the recoiling side against the single tags as following

$$N^{\bar{D}^0}_{D^0_{tag}} = N_{D^0_{tag}} \times (1 - \xi), \qquad N^{D^-}_{D^0_{tag}} = N_{D^0_{tag}} \times \xi,$$

$$N^{\bar{D}^0}_{D^+_{tag}} = N_{D^+_{tag}} \times \beta, \qquad N^{D^-}_{D^+_{tag}} = N_{D^+_{tag}} \times (1 - \beta).$$

Where ξ and β are two parameters. They are functions of $\sigma_{D^+ D^{*-}}$, $\sigma_{D^{*+} D^{*-}}$, $\sigma_{D^0 \bar{D}^{*0}}$, $\sigma_{D^{*0} \bar{D}^{*0}}$ and $BF(D^{*\pm} \rightarrow \pi^{\pm} D^0)$. ($\xi$=0.1768$\pm$0.0175, β=0.5460$\pm$0.0622. For more details, please refer to reference [2])

3 Single Tag for D^0 and D^+

In the single tag analysis, data from the Main Drift Chamber(MDC), the Time-Of-Flight system and dE/dx system are used.Programme PARTID1 is used to do π/K identification.

For each event we require that at least 2 (but not more than 10) charged tracks were well reconstructed in MDC (i.e. $M_{fit} = 2$ or -19 or -9). Except for tracks from K_s^0 decay, each track is required to have impact parameter less than 1.0 cm in the xy plane and the mutual Z difference between the charged tracks should be less than 3 cm. In addition, in order to optimize the momentum resolution and charged particle identification, a geometry cut ($\mid cos\theta \mid \leq 0.8$, where the θ is polar angle of the track) is applied. For the charged particle mass assignment, two levels of particle identification are applied. First a combined particle confidence level calculated using the dE/dx and TOF measurements is required to be greater than 1% for $K(\pi)$ hypothesis; then a normalized likelihood ratio $LR(K)_{TOF+dEdx} > LR(\pi)_{TOF+dEdx}$ ($LR(\pi)_{TOF+dEdx} > LR(K)_{TOF+dEdx}$) is required for the $K(\pi)$ hypothesis. If the track pass the two level cuts, the $K(\pi)$ mass is assigned to the track.

After the particle mass assignments, an invariant mass of different combinations for the four hadronic decay modes are calculated using corrected momenta components for a small value of shift of magnetic field and ionization loss of the particle in the material interior to the MDC gas.

Figure 3.1 shows a scatter plot of the total momenta as a function of the invariant mass of the $K^\pm\pi^\mp$. There are three enhanced clusters. Each of them corresponds to the neutral D mesons coming from the three pairs of the D^*D^*, the DD^* and the $D\bar{D}$, respectively.

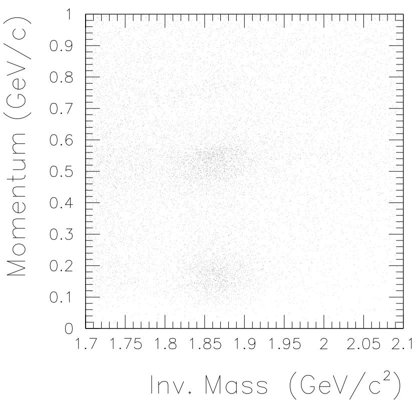

Fig.3.1: Momenta as a function of the $K^\mp\pi^\pm$ combinations for events for which the charged tracks passed the selection criteria.

Fig.3.2-Fig.3.4 are the momentum distribution of singly tagged D mesons whose invariant mass are confined to a window of $\pm 3\sigma_{m_{D^0}}$ (or $\pm 3\sigma_{m_{D^+}}$) cuts of the nominal D^0 meson (or D^+) mass for $D^0 \to K^-\pi^+$, $D^0 \to K^-\pi^+\pi^+\pi^-$, $D \to K^-\pi^+\pi^+$ channels. A binned maximum-likelihood fit (all fit parameters are free to be adjusted) to these momentum spectra with three Gaussian functions and three order polynomial background[1] yields mean momenta and widths for each of the three decay modes. Table 3.1 summarizes the fitted results of the first two peaks for each decay mode.

[1]BWGFIT package, BES physics analysis software.

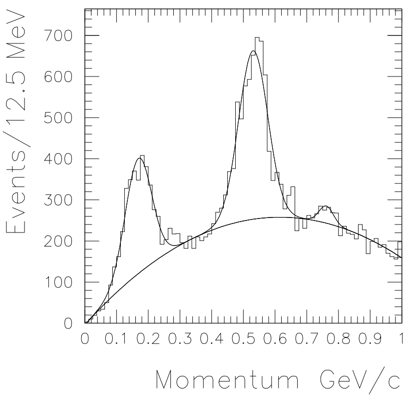

Fig.3.2: Momentum distribution of the $K^{\mp}\pi^{\pm}$ combinations for events for which the charged tracks passed the selection criteria.

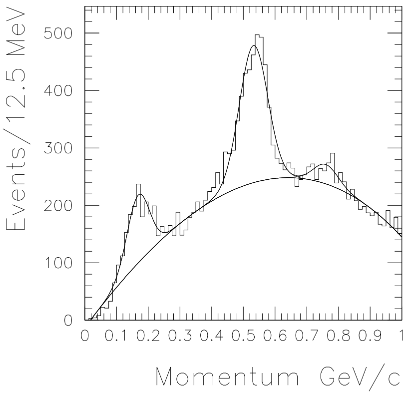

Fig.3.3: Momentum distribution of the $K^{\mp}\pi^{\pm}\pi^{\pm}\pi^{\mp}$ combinations for events for which the charged tracks passed the selection criteria.

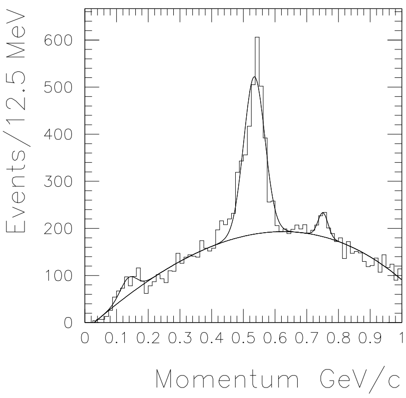

Fig.3.4: Momentum distribution of the $K^{\mp}\pi^{\pm}\pi^{\pm}$ combinations for events for which the charged tracks passed the selection criteria.

Table 3.1 Summary of result fitted to momentum spectra of D mesons

Decay Modes	P (GeV/c) (D from D^*D^*)	σ_P (GeV/c)	P (GeV/c) (D from DD^*)	σ_P (GeV/c)
$D^0 \to K^{\pm}\pi^{\mp}$	0.162 ± 0.001	0.044 ± 0.001	0.531 ± 0.001	0.046 ± 0.001
$D^0 \to K^{\pm}\pi^{\mp}\pi^{\mp}\pi^{\pm}$	0.168 ± 0.03	0.035 ± 0.002	0.532 ± 0.045	0.045 ± 0.003
$D^{\pm} \to K^{\pm}\pi^{\mp}\pi^{\mp}$	0.137 ± 0.046	0.026 ± 0.029	0.534 ± 0.002	0.034 ± 0.001

For figures of invariant mass distribution for the four channels, see section 5.

4 Particle identification efficiencies and misidentification rates for charged tracks against single tags

For tracks against D single tags, the programme of PARTID2 is used. We will discuss the dependence on transverse momentum P_{xy}(instead of on momentum) of particle identification efficiencies and misidentification rates.

4.1 Criteria of particle identification for charged tracks against single tags

The criteria of particle identification for charged tracks against single tags is a bit different from those for charged tracks that combined the single tags, and the difference can be stated as follows. First a combined particle confidence level calculated using the dE/dx, TOF and BSC measurements is also required to be greater than 1% for $e/K/\pi$ hypothesis; then if the confidence level $CL(e)_{TOF+dEdx+BSC} > CL(\pi)_{TOF+dEdx+BSC}$ and $CL(e)_{TOF+dEdx+BSC} > CL(K)_{TOF+dEdx+BSC}$, we call this track an electron. Second if the program of muonid says one particle is a muon, the TOF, dEdx and BSC information didn't tell it is an electron, and the confidence level extracted from dE/dx, TOF and BSC information have $CL(K)_{TOF+dEdx+BSC} < 2CL(\pi)_{TOF+dEdx+BSC}$ and $CL(K)_{TOF+dEdx+BSC} < 2CL(\mu)_{TOF+dEdx+BSC}$ we call it a muon. Third once a track is called a muon, it can neither be a π nor a K. Fourth,we strictly confine our discussion for tracks in the recoiling side to those tracks which have impact parameter less than 0.4 cm. Fifth, we strictly confine our discussion for tracks in the recoiling side to those tracks which have $\mid cos\theta \mid \leq 0.6$ for sake of the geometrical parameters of muon counter. Sixth, we only care about those charged tracks in the recoiling side with transverse momentum greater than 0.52 GeV/c. Muons with P_{xy} less than 0.52 GeV/c can not hit muon counter and can't be distinguished from pions by other sub-detectors, thus in noway can be considered by BES detector.

4.2 Data sample and $\eta^{a-b(i)}$

In the following tables we divide transverse momentum interval from 0.52 GeV/c to 1.02 GeV/c into ten subintervals, each with width 0.05 GeV/c and calculate related quantities interval by interval.

Define $\eta^{a-b(i)}$ the probability of identifying particle a as b in P_{xy} interval from $(0.52 + (i-1) \times 0.05)$GeV/c to $(0.52 + i \times 0.05)$GeV/c, where a and b can be e, μ, π or K. In order to obtain $\eta^{a-b}(i)$, we use real e, μ and π sample data and MC pure K sample data to pass our particle identification programme. In Table 4.1 we use Cosmic ray as muon sample. In table 4.2 we use π samples from process of $J/\psi \to \omega\pi\pi$ and $J/\psi \to \omega\pi\pi\pi\pi$. In table 4.4 we use radiative Bhabha as e samples. In table 4.3 we use Monto-Carlo K sample to study $\eta^{K-b(i)}$, since it is very difficult to obtain enough pure real kaon data sample. We emphsize again that all tracks selected in table 4.1-4.4 have abs(cosθ).lt.0.6.

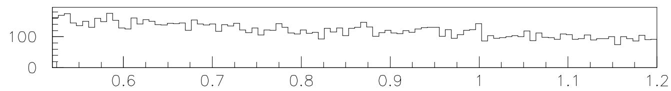

Fig 4.1 Pxy Distribution of Cosmic Ray,input

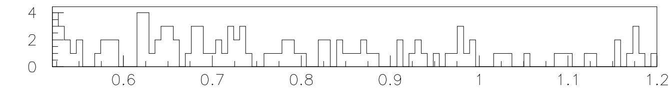

Fig 4.2 Pxy Distribution of Cosmic Ray,identified as e

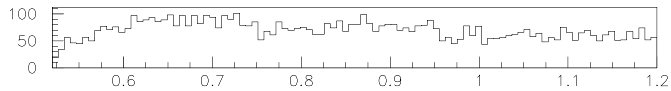

Fig 4.3 Pxy Distribution of Cosmic Ray,identified as mu

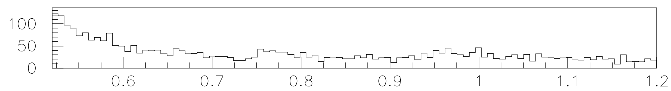

Fig 4.4 Pxy Distribution of Cosmic Ray,identified as pi

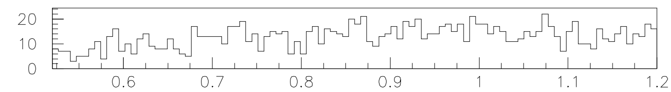

Fig 4.5 Pxy Distribution of Cosmic Ray,identified as k

Figure 4.1 is the transverse momentum distribution of input cosmic ray tracks. We have about 7000 well reconstructed tracks of muons in the interval from 0.52 GeV/c to 1.02 GeV/c, and the numbers of tracks in each subintervals are listed in table as $N^{input(i)}$. Transverse momentum distribution of particles which are identified as e, μ, π, K are shown in figures 4.2, 4.3, 4.4, and 4.5 separately. And the numbers in each interval are listed in table 4.1 as $N^{\mu-e(i)}$, $N^{\mu-\mu(i)}$, $N^{\mu-\pi(i)}$, $N^{\mu-K(i)}$ separately. Thus $\eta^{\mu-e(i)}$,$\eta^{\mu-\mu(i)}$ $\eta^{\mu-\pi(i)}$ and $\eta^{\mu-K(i)}$ in each interval can easily be calculated. The subsequent discussion for the results from real π sample data, MC pure K sample data, and real e samples are parallel to that of Figure 4.1-4.5 and table 4.1. The results are shown in Fig 4.6-4.20 and table 4.2-4.4.

Table 4.1 On the P_{xy} dependence of η^{a-b} . Use Cosmic Ray as μ sample data.

P_{xy}	.52-.57	.57-.62	.62-.67	.67-.72	.72-.77	.77-.82	.82-.87	.87-.92	.92-.97	.97-1.02
$N^{input(i)}$	1136	1090	1064	1004	912	881	883	867	896	799
$N^{\mu-e(i)}$	12	9	17	13	10	7	9	6	6	8
$N^{\mu-\mu(i)}$	339	564	658	656	561	535	569	578	516	432
$N^{\mu-\pi(i)}$	674	397	273	214	206	225	170	164	230	220
$N^{\mu-K(i)}$	47	69	73	88	105	87	115	101	121	119
$\eta^{\mu-e(i)}$	0.011 $\pm$0.003	0.008 $\pm$0.003	0.016 $\pm$0.004	0.013 $\pm$0.004	0.011 $\pm$0.003	0.008 $\pm$0.003	0.010 $\pm$0.003	0.007 $\pm$0.003	0.007 $\pm$0.003	0.010 $\pm$0.004
$\eta^{\mu-\mu(i)}$	0.298 $\pm$0.016	0.517 $\pm$0.022	0.618 $\pm$0.024	0.653 $\pm$0.025	0.615 $\pm$0.026	0.607 $\pm$0.026	0.644 $\pm$0.027	0.667 $\pm$0.028	0.576 $\pm$0.025	0.541 $\pm$0.026
$\eta^{\mu-\pi(i)}$	0.593 $\pm$0.023	0.364 $\pm$0.018	0.257 $\pm$0.016	0.213 $\pm$0.015	0.226 $\pm$0.016	0.255 $\pm$0.017	0.193 $\pm$0.015	0.189 $\pm$0.015	0.257 $\pm$0.017	0.275 $\pm$0.019
$\eta^{\mu-K(i)}$	0.041 $\pm$0.006	0.063 $\pm$0.008	0.069 $\pm$0.008	0.088 $\pm$0.009	0.115 $\pm$0.011	0.099 $\pm$0.011	0.130 $\pm$0.012	0.116 $\pm$0.012	0.135 $\pm$0.012	0.149 $\pm$0.014

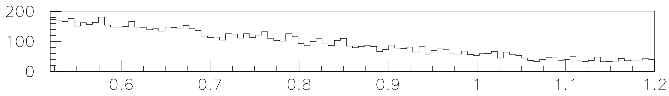

Fig 4.6 Pxy Distribution of pi sample,input

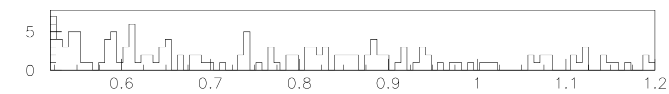

Fig 4.7 Pxy Distribution of pi sample,identified as e

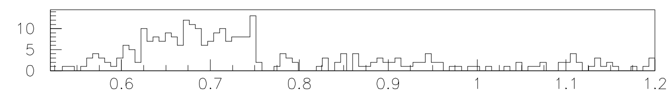

Fig 4.8 Pxy Distribution of pi sample,identified as mu

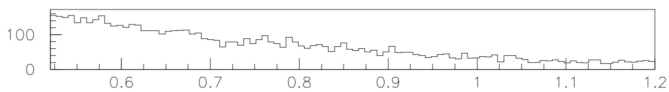

Fig 4.9 Pxy Distribution of pi sample,identified as pi

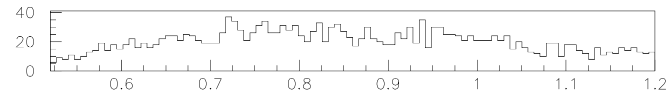

Fig 4.10 Pxy Distribution of pi sample,identified as k

Table 4.2 and Figure 4.6-4.10 are parallel to table 4.1 and Figure 4.1-4.5 but for π samples. The π data samples are selected from decay process of $J/\psi \to \omega\pi\pi$ and $J/\psi \to \omega\pi\pi\pi\pi$ by the kinematic fitting method.

Table 4.2 On the P_{xy} dependence of η^{a-b}. Use $J/\psi \to \omega\pi\pi$ and $J/\psi \to \omega\pi\pi\pi\pi$ as π sample data.

P_{xy}	.52-.57	.57-.62	.62-.67	.67-.72	.72-.77	.77-.82	.82-.87	.87-.92	.92-.97	.97-1.02
$N^{input(i)}$	1225	1150	1057	928	885	763	699	583	535	433
$N^{\pi-e(i)}$	26	21	14	7	11	12	12	13	9	5
$N^{\pi-\mu(i)}$	8	24	56	70	43	10	15	14	14	5
$N^{\pi-\pi(i)}$	1096	961	821	672	600	535	464	387	308	260
$N^{\pi-K(i)}$	71	126	152	164	215	198	197	161	194	160
$\eta^{\pi-e(i)}$	0.021 $\pm$0.004	0.018 $\pm$0.004	0.013 $\pm$0.004	0.008 $\pm$0.003	0.012 $\pm$0.004	0.016 $\pm$0.005	0.017 $\pm$0.005	0.022 $\pm$0.006	0.017 $\pm$0.006	0.012 $\pm$0.005
$\eta^{\pi-\mu(i)}$	0.007 $\pm$0.002	0.021 $\pm$0.004	0.053 $\pm$0.007	0.075 $\pm$0.009	0.049 $\pm$0.007	0.013 $\pm$0.004	0.021 $\pm$0.005	0.024 $\pm$0.006	0.026 $\pm$0.007	0.012 $\pm$0.005
$\eta^{\pi-\pi(i)}$	0.895 $\pm$0.027	0.836 $\pm$0.027	0.777 $\pm$0.027	0.724 $\pm$0.028	0.678 $\pm$0.028	0.701 $\pm$0.030	0.664 $\pm$0.031	0.664 $\pm$0.034	0.576 $\pm$0.033	0.600 $\pm$0.037
$\eta^{\pi-K(i)}$	0.058 $\pm$0.007	0.110 $\pm$0.010	0.144 $\pm$0.012	0.177 $\pm$0.014	0.243 $\pm$0.017	0.260 $\pm$0.018	0.282 $\pm$0.020	0.276 $\pm$0.022	0.363 $\pm$0.026	0.370 $\pm$0.029

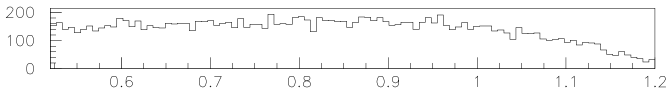

Figure 4.11 Pxy distribution of MC k,input

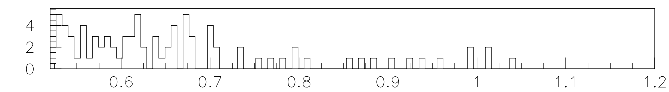

Figure 4.12 Pxy distribution of MC k,identified as e

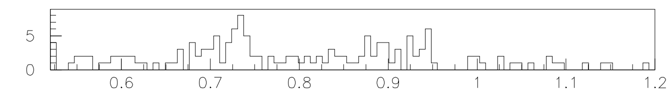

Figure 4.13 Pxy distribution of MC k,identified as mu

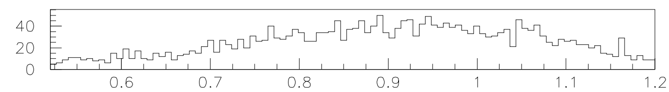

Figure 4.14 Pxy distribution of MC k,identified as pi

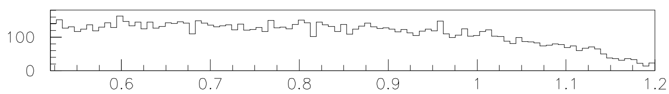

Figure 4.15 Pxy distribution of MC k,identified as k

Table 4.3 On the P_{xy} Dependence of η^{a-b} . Use M.C pure K as K sample data.

P_{xy}	.52-.57	.57-.62	.62-.67	.67-.72	.72-.77	.77-.82	.82-.87	.87-.92	.92-.97	.97-1.02
$N^{input(i)}$	1074	1154	1126	1176	1174	1214	1226	1259	1206	1088
$N^{K-e(i)}$	21	19	16	12	4	4	1	3	3	4
$N^{K-\mu(i)}$	11	11	7	19	28	10	12	21	17	5
$N^{K-\pi(i)}$	64	88	89	151	188	228	261	290	308	264
$N^{K-K(i)}$	971	1033	1008	991	950	965	951	941	874	812
$\eta^{K-e(i)}$	0.020 $\pm$0.004	0.016 $\pm$0.004	0.014 $\pm$0.004	0.010 $\pm$0.003	0.003 $\pm$0.002	0.003 $\pm$0.002	0.001 $\pm$0.001	0.002 $\pm$0.002	0.002 $\pm$0.001	0.004 $\pm$0.002
$\eta^{K-\mu(i)}$	0.010 $\pm$0.003	0.010 $\pm$0.003	0.006 $\pm$0.002	0.016 $\pm$0.004	0.024 $\pm$0.005	0.008 $\pm$0.003	0.010 $\pm$0.003	0.017 $\pm$0.004	0.014 $\pm$0.003	0.005 $\pm$0.002
$\eta^{K-\pi(i)}$	0.060 $\pm$0.007	0.076 $\pm$0.008	0.079 $\pm$0.008	0.128 $\pm$0.010	0.160 $\pm$0.012	0.188 $\pm$0.012	0.213 $\pm$0.013	0.230 $\pm$0.014	0.255 $\pm$0.015	0.243 $\pm$0.015
$\eta^{K-K(i)}$	0.904 $\pm$0.029	0.895 $\pm$0.028	0.895 $\pm$0.028	0.843 $\pm$0.027	0.809 $\pm$0.026	0.795 $\pm$0.026	0.776 $\pm$0.025	0.747 $\pm$0.024	0.725 $\pm$0.025	0.746 $\pm$0.026

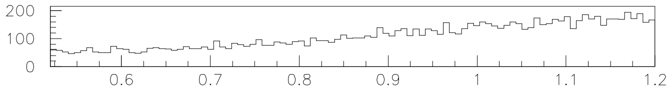

Figure 4.16 Pxy distribution of radiative Bhabha,input

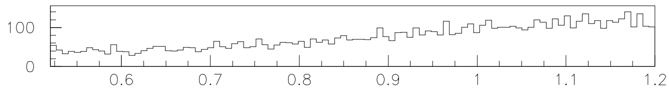

Figure 4.17 Pxy distribution of radiative Bhabha,identified as e

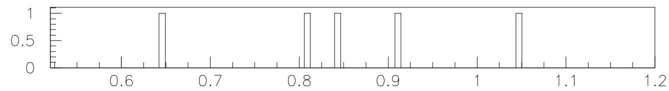

Figure 4.18 Pxy distribution of radiative Bhabha,identified as mu

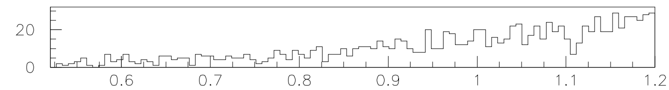

Figure 4.19 Pxy distribution of radiative Bhabha,identified as pi

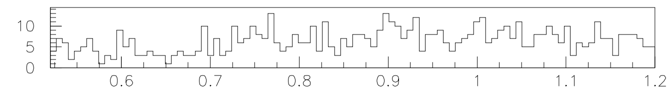

Figure 4.20 Pxy distribution of radiative Bhabha,identified as k

In table 4.4 and Figure 4.16-4.20, we illustrate you the result from radiative Bhabha. We have over 6000 e sample tracks with P_{xy} greater than 0.52 GeV/c, and only five tracks are identified as muons. In general $\eta^{e-\mu(i)}$ is less than 0.2 percent.

Table 4.4 On the P_{xy} Dependence of η^{a-b} . Use radiative Bhabha as e sample data.

P_{xy}	.52-.57	.57-.62	.62-.67	.67-.72	.72-.77	.77-.82	.82-.87	.87-.92	.92-.97	.97-1.02
$N^{input(i)}$	413	426	448	524	581	642	724	883	937	1059
$N^{e-e}(i)$	308	289	323	362	411	442	505	584	659	741
$N^{e-\mu(i)}$	0	0	1	0	0	1	1	1	0	0
$N^{e-\pi(i)}$	10	15	7	13	12	20	29	35	38	33
$N^{e-K(i)}$	21	15	17	15	25	15	10	15	11	5
$\eta^{e-e(i)}$	0.746 $\pm$0.042	0.678 $\pm$0.040	0.721 $\pm$0.040	0.691 $\pm$0.036	0.707 $\pm$0.035	0.688 $\pm$0.033	0.698 $\pm$0.031	0.661 $\pm$0.027	0.703 $\pm$0.027	0.700 $\pm$0.026
$\eta^{e-\mu(i)}$	0.000 $\pm$0.000	0.000 $\pm$0.000	0.002 $\pm$0.002	0.000 $\pm$0.000	0.000 $\pm$0.000	0.002 $\pm$0.002	0.001 $\pm$0.001	0.001 $\pm$0.001	0.000 $\pm$0.000	0.000 $\pm$0.000
$\eta^{e-\pi(i)}$	0.024 $\pm$0.008	0.035 $\pm$0.009	0.016 $\pm$0.006	0.025 $\pm$0.007	0.021 $\pm$0.006	0.031 $\pm$0.007	0.040 $\pm$0.007	0.040 $\pm$0.007	0.041 $\pm$0.007	0.031 $\pm$0.005
$\eta^{e-K(i)}$	0.051 $\pm$0.011	0.035 $\pm$0.009	0.038 $\pm$0.009	0.029 $\pm$0.007	0.043 $\pm$0.009	0.023 $\pm$0.006	0.014 $\pm$0.004	0.017 $\pm$0.004	0.012 $\pm$0.004	0.005 $\pm$0.002

5 Double Tags

For D^+ (D^0) single tag we define invariant mass interval from 1.869-3σ_{M_D} (1.864-3σ_{M_D}) to 1.869+3σ_{M_D} (1.864+3σ_{M_D}) as signal region denoted as region A. In the figures of 5.1-5.4, the regions denoted as region B and C which are outside the signal region A are defined as side bands to evaluate the muons which come from background.

The information of charg sign of charged tracks is extremly well reconstructed in BES data, so only the same charge sign of electrons, muons, pions and kaons can be misidentified as each other. So in this paper we define electrons, pions and kaons with the same charge sign with right sign muons as right sign electrons, pions and kaons. Electrons, pions and kaons with the same charge sign with wrong sign muons are called wrong sign electrons,pions and kaons.

For the measurement of the inclusive semi-muonic decay branching fractions of the charged and neutral D mesons, one need to search for candidate e, μ , π, K in the recoiling side against tagged D mesons and to unfold the numbers into numbers of real e, μ, π, K. In the analysis the candidate electrons,muons,pions and kaons are searched for by using the criteria stated in section 4, thus the particle identification efficiencies and misidentification rates valid for our following discussion.

We use the criteria stated in section 4 to search for candidate e, μ , π, K in the recoiling side against tagged events in signal region and side bands. Figure.5.5 shows a combined invariant mass of the Knπ (where n=1,2,3) for the four modes together for events for which one candidate μ was observed in the recoil. Suppose in transverse momentum interval from $(0.52+0.05\times(i-1))$ GeV/c to $(0.52+0.05\times i)$ GeV/c, we observed $N^{e(i)}_{obsr(sig)}$ right candidate electrons, $N^{\mu(i)}_{obsr(sig)}$ right sign candidate muons, $N^{\pi(i)}_{obsr(sig)}$ right sign candidate pions and $N^{K(i)}_{obsr(sig)}$ right sign candidate kaons among the well reconstructed charged tracks in the recoiling side against single D tags in signal region. We also assume that there are $N^{e(i)}_{realr(sig)}$ real electrons, $N^{\mu(i)}_{realr(sig)}$ real muons, $N^{\pi(i)}_{realr(sig)}$ real pions and $N^{K(i)}_{realr(sig)}$ real kaons among those well reconstructed tracks, where the upper script (i) stand for the number of subinterval. The candidate electrons have four components:one is real electrons, others are muons, pions and kaons that are misidentified as electrons. Similarly for the observed candidate μ, π and K, they also have four components. Thus we have

$$N^{e(i)}_{obsr(sig)} = N^{e(i)}_{realr(sig)}\times\eta^{e-e(i)}+N^{\mu(i)}_{realr(sig)}\times\eta^{\mu-e(i)}+N^{\pi(i)}_{realr(sig)}\times\eta^{\pi-e(i)}+N^{K(i)}_{realr(sig)}\times\eta^{K-e(i)} \quad (5)$$

$$N^{\mu(i)}_{obsr(sig)} = N^{e(i)}_{realr(sig)}\times\eta^{e-\mu(i)}+N^{\mu(i)}_{realr(sig)}\times\eta^{\mu-\mu(i)}+N^{\pi(i)}_{realr(sig)}\times\eta^{\pi-\mu(i)}+N^{K(i)}_{realr(sig)}\times\eta^{K-\mu(i)} \quad (6)$$

$$N^{\pi(i)}_{obsr(sig)} = N^{e(i)}_{realr(sig)}\times\eta^{e-\pi(i)}+N^{\mu(i)}_{realr(sig)}\times\eta^{\mu-\pi(i)}+N^{\pi(i)}_{realr(sig)}\times\eta^{\pi-\pi(I)}+N^{K(i)}_{realr(sig)}\times\eta^{K-\pi(i)} \quad (7)$$

$$N^{K(i)}_{obsr(sig)} = N^{e(i)}_{realr(sig)}\times\eta^{e-K(i)}+N^{\mu(i)}_{realr(sig)}\times\eta^{\mu-K(i)}+N^{\pi(i)}_{realr(sig)}\times\eta^{\pi-K(i)}+N^{K(i)}_{realr(sig)}\times\eta^{K-K(i)} \quad (8)$$

With equation (5), (6), (7) and (8) combined,the numbers of candidate electrons, muons, pions and kaons can easily be unfolded into the numbers of true electrons, muons, pions and kaons. And the total number of true muons in signal region is:

$$N^{\mu}_{realr(sig)} = \Sigma N^{\mu(i)}_{realr(sig)} \quad (9)$$

The same discussion are also valid for the events observed in the side bands:

$$N^{e(i)}_{obsr(sid)} = N^{e(i)}_{realr(sid)}\times\eta^{e-e(i)}+N^{\mu(i)}_{realr(sid)}\times\eta^{\mu-e(i)}+N^{\pi(i)}_{realr(sid)}\times\eta^{\pi-e(i)}+N^{K(i)}_{realr(sid)}\times\eta^{K-e(i)} \quad (10)$$

$$N^{\mu(i)}_{obsr(sid)} = N^{e(i)}_{realr(sid)}\times\eta^{e-\mu(i)}+N^{\mu(i)}_{realr(sid)}\times\eta^{\mu-\mu(i)}+N^{\pi(i)}_{realr(sid)}\times\eta^{\pi-\mu(i)}+N^{K(i)}_{realr(sid)}\times\eta^{K-\mu(i)} \quad (11)$$

$$N^{\pi(i)}_{obsr(sid)} = N^{e(i)}_{realr(sid)} \times \eta^{e-\pi(i)} + N^{\mu(i)}_{realr(sid)} \times \eta^{\mu-\pi(i)} + N^{\pi(i)}_{realr(sid)} \times \eta^{\pi-\pi(I)} + N^{K(i)}_{realr(sid)} \times \eta^{K-\pi(i)} \quad (12)$$

$$N^{K(i)}_{obsr(sid)} = N^{e(i)}_{realr(sid)} \times \eta^{e-K(i)} + N^{\mu(i)}_{realr(sid)} \times \eta^{\mu-K(i)} + N^{\pi(i)}_{realr(sid)} \times \eta^{\pi-K(i)} + N^{K(i)}_{realr(sid)} \times \eta^{K-K(i)} \quad (13)$$

And the total number of true muons observed in the side bands(lower and higher side bands)is:

$$N^{\mu}_{realr(sid)} = \Sigma N^{\mu(i)}_{realr(sid)} \quad (14)$$

We can use the following equation to obtain the number of net right sign muons directly from D^+(or D^0)mesons:

$$N^{\mu}_{netr} = N^{\mu}_{realr(sig)} - \alpha N^{\mu}_{realr(sid)},$$

where α is the ratio of background entries in singly tagged signal region to that in the side bands .

In the same way as that we did for unfolding the number of right sign muons, we can obtain the number of net wrong sign muons N^{μ}_{netw}. The results are summarized in table 5.1.

Table 5.1 Summary of All Single Tags and the number of μ found in recoiling side.(RS stands for right sign while WS for wrong sign)

decay mode	Inv. Mass	No. of Single Tag	No. of μ (RS)	No. of μ(WS)
$D^0 \to K^-\pi^+$	1.8656 ± 0.0007	3274 ± 173	51.43 ± 7.6	-0.76
$D^0 \to K^-\pi^+\pi^+\pi^-$	1.8646 ± 0.0006	2598 ± 190	38.59 ± 6.7	1.03
$D^+ \to K^-\pi^+\pi^+$	1.8685 ± 0.0008	1896 ± 151	34.88 ± 5.9	1.22
$D^+ \to K^0\pi^+$	1.8696 ± 0.0029	172 ± 38	5.03 ± 2.2	-0.62

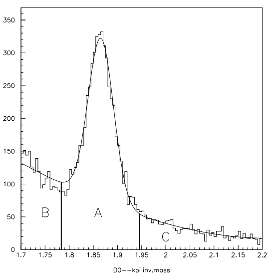

Fig.5.1: Invariant mass distribution of the $K^{\mp}\pi^{\pm}$ combinations fo which the total momenta are within $\pm 3\sigma_P$.α=0.7119.

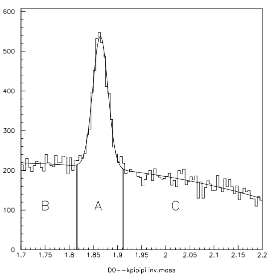

Fig.5.2: Invariant mass distribution of $K^{\mp}\pi^{\pm}\pi^{\pm}\pi^{\mp}$ combinations for which the total momenta are within $\pm 3\sigma_P$, α=0.2568.

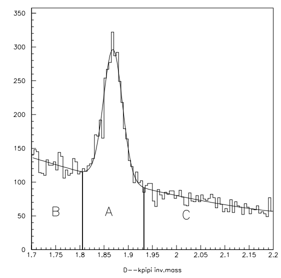

Fig.5.3: Invariant mass distribution of $K^{\mp}\pi^{\pm}\pi^{\pm}$ combinations for which the total momenta are within $\pm 3\sigma_P$. α=0.40896.

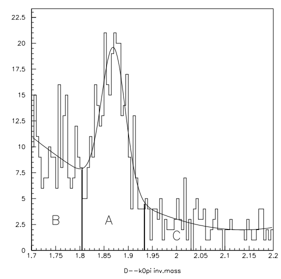

Fig.5.4: Invariant mass distribution of $K^0\pi^+$ combinations for which the total momenta are within $\pm 3\sigma_P$. α=0.4269.

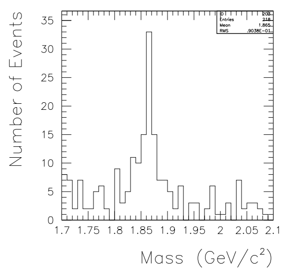

Fig.5.5: Invariant mass distribution of Knπ combinations for which one candidate μ was observed in the recoil.

6 Acceptance of true muons in the recoiling side against D tags

From now on, we have calculated the number of muons in the recoiling side against D^0 or D^+ single tag. Actually they are the numbers of muons which have $|\cos\theta|<0.6$, rxy<0.4 cm, and which are tracked successfully. Also only $P_{xy}>0.52$ GeV/c tracks of muons can be identified as muons. We have to know the efficiencies of these cuts in order to know the numbers of true muons produced against D^0 or D^+ single tags.

The way of determining these efficiencies is to produce Monte Carlo DD^* and D^0D^{*0} events with one D decaying into one of our singly tagged channel and the other D decaying into μX and to treat them as if they were real data. From the Monto-Carlo kinematic simulation we can know two ratios of number of μ with $P_{xy}>0.52$ GeV/c to number of all μ produced in the recoiling side against D^+ single tags and D^0 single tag, respectively.

6.1 The P_{xy} spectrum for μ from direct D and indirect D

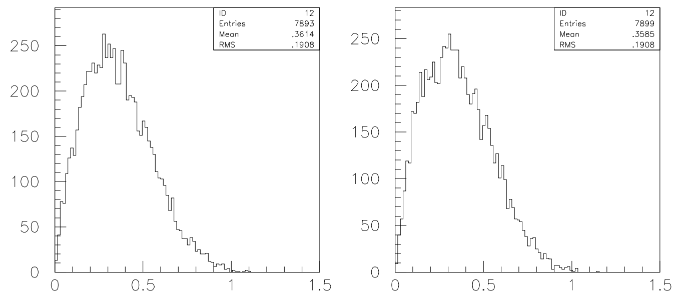

Fig6.1 Pt Distribution of mu from direct D0 Fig6.2 Pt Distribution of mu from indirect D0

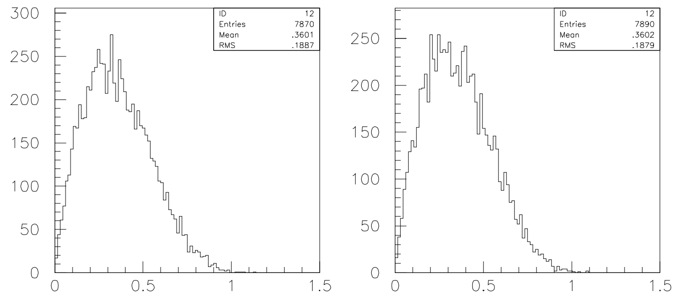

Fig6.3 Pt Distribution of mu from direct D Fig6.4 Pt Distribution of mu from indirect D

Fig.6.1-6.2 are transverse momentum spectrums for μ from direct D^0 and indirect D^0. Fig.6.3-6.4 are transverse momentum spectrums for μ from direct D^+(or D^-) and indirect D^+(or D^-). From the four figures we know that the portion of muons which has P_{xy} greater than 0.52 GeV among all the muons are all equal to $(20.4 \pm 0.2)\%$, directly or indirectly from D or D^0.

6.2 Efficiency of Tracking, Vertex cut, Geometrical cut and P_{xy} cut

Define $\epsilon_{D\rightarrow\mu X}$ the efficiency of tracking, vertex cut and geometrical cut in finding muons in the recoil side against D mesons. What we have to do next in this section is very similar to what we have done in section 4 and section 5. First we use MC data as μ, π and e samples to determine particle identification efficiencies and misidentification rates for charged tracks. Second we need to use these identification efficiencies and misidentification rates from MC data to analyze the 'double tags' of DD* produced from MC simulation. The numbers of single tags and the numbers of muons found in the recoil side are listed in table 6.1, which is parallel to table 5.1. In this section DD* stands for charged pair.

Table 6.1 Summary of All Single Tags and μ No. found in recoiling side.

Decay mode	N_{DD^*}	No. of Single Tag	N^{μ}_{netr}
D^0D^{*0}, $D^0 \to K^-\pi^+$, $D^{*0} \to \mu X$	8000	5725.0 ± 79.0	921.0 ± 30.2
D^0D^{*0},$D^{*0} \to K^-\pi^+$+γ (or $\pi 0$),$D \to \mu X$	8000		
DD^*,$D^* \to D^0$+π,$D^0 \to K^-\pi^+$,$D^0 \to \mu X$	8000	2947.0 ± 70	493.0 ± 28.0
D^0D^{*0},$D^0 \to K^-\pi^+\pi^+\pi^-$,$D^{*0} \to \mu X$	8000	3592.0 ± 65.0	532.0 ± 26.0
D^0D^{*0},$D^{*0} \to K^-\pi^+\pi^+\pi^-$+$\gamma$ (or $\pi 0$),$D^0 \to \mu X$	16000		
DD^*,$D^* \to D^0$+π, $D^0 \to K^-\pi^+\pi^+\pi^-$,$D \to \mu X$	8000	1175.0 ± 37.2	189.0 ± 15.0
DD^*,$D^+ \to K^-\pi^+\pi^+$,$D^{*-} \to \mu X$	8000	4079.5 ± 72.0	635.9 ± 28.3
DD^*,$D^* \to K^-\pi^+\pi^+$+γ(or $\pi 0$),$D \to \mu X$	8000		
DD^*,$D \to K^-\pi^+\pi^+$,$D^* \to \pi$+D^0,$D^0 \to \mu X$	8000	1941.4 ± 47.6	301.8 ± 21
Total	80000	19460.0 ± 155.3	3072.7 ± 61.8

In general, we get 19460 (D^+ or D^0) single tags,and we find 3072.7 muons in the recoil side. Thus the average efficiency $\epsilon_{D\to\mu X}$ is 3072.7/19460.0=$(15.79 \pm 0.43)\%$.

7 Results

7.1 Inclusive decay branching fractions

Monte carlo study shows that the probability of $D^{-'}s$ appearance in the recoiling side of a D^0 tag $\xi = 0.1768 \pm 0.0175$ while the probability of $\bar{D}^0$'s appearance in the recoiling side of a D^+ tag $\beta = 0.5460 \pm 0.0622$. Inserting the numbers of the events observed for the single and 'double' tags and the efficiencies $\epsilon_{D\to\mu X}$ into formula (3) and (4), we obtain the inclusive semi-muonic decay branching fractions of

$$BF(D^+ \to \mu^+ X) = (17.17 \pm 6.08)\%$$

and

$$BF(D^0 \to \mu^+ X) = (8.11 \pm 2.08)\%,$$

where the errors are statistical.

7.2 Likelihood Statistical Analysis

In this section we use a Likelihood statistical analysis method to determine the decay branching fractions to obtain a best estimation.

After a little variable substitution the formula (3) and (4) can be rewritten into

$$N^{\mu\ X}_{D^0_{tag}} = \frac{N_{D^0_{tag}}}{1-\beta} \times \left(\frac{\xi \times N^{\mu\ X}_{D^+_{tag}}}{N_{D^+_{tag}}} + \epsilon \times (1-\beta-\xi)BF(D^0 \to \mu^+ X)\right) \tag{15}$$

$$N^{\mu\ X}_{D^+_{tag}} = \frac{N_{D^+_{tag}}}{1-\xi} \times \left(\frac{\beta \times N^{\mu\ X}_{D^0_{tag}}}{N_{D^0_{tag}}} - \epsilon \times (1-\beta-\xi)BF(D^+ \to \mu^+ X)\right) \tag{16}$$

where $N^{\mu\ X}_{D^0_{tag}}$ and $N^{\mu\ X}_{D^+_{tag}}$ are numbers of inclusive μ events observed in the recoil system. Since the numbers of single tagged neutral and charged D mesons are large compared to the numbers of the inclusive μ events observed, we take the number of the single tagged D mesons as two constants. We construct a joint likelihood function , which is a product of two likelihood functions described the probabilities of observing the inclusive μ events in the recoiling side against the tagged neutral and charged D mesons, to fluctuate the numbers of inclusive μ events observed.

The probability functions for the inclusive μ events appeared in the recoiling side against tagged neutral and charged D mesons are given by

$$P^{\mu X}_{D^+_{tag}} = \frac{1}{\sqrt{2\pi}\sigma_{N^{\mu X}_{D^+_{tag}}}} e^{-(N^{\mu X}_{D^+_{tag}} - n^{\mu X}_{D^+_{tag}})^2/2\sigma^2_{N^{\mu X}_{D^+_{tag}}}}$$

and

$$P^{\mu X}_{D^0_{tag}} = \frac{1}{\sqrt{2\pi}\sigma_{N^{\mu X}_{D^0_{tag}}}} e^{-(N^{\mu X}_{D^0_{tag}} - n^{\mu X}_{D^0_{tag}})^2/2\sigma^2_{N^{\mu X}_{D^0_{tag}}}},$$

respectively, where $n^{\mu X}_{D^+_{tag}}$ and $n^{\mu X}_{D^0_{tag}}$ are parameters to be estimated for the numbers of the inclusive μ events appeared in the recoil side against the tagged neutral and charged D mesons.From the two probability functions we construct a joint likelihood function, which is a product of two likelihood functions described the probabilities of observing the inclusive μ events in the recoiling side against the tagged neutral and charged D mesons, to fluctuate the numbers of the inclusive μ events observed. The log-likelihood function is:

$$lnL(N^{\mu X}_{D^+_{tag}}, n^{\mu X}_{D^+_{tag}}, N^{\mu X}_{D^0_{tag}}, n^{\mu X}_{D^0_{tag}}) = ln(P^{\mu X}_{D^+_{tag}} \times P^{\mu X}_{D^0_{tag}}).$$

Using the relation of decay branching fraction (3) and (4), the numbers of the inclusive μ events observed in the recoil side, the constants for the single tags, efficiency and parameters ξ and β, for a given values of the decay branching fraction, the log-likelihood function lnL is maximized by varying the two parameters $n^{\mu X}_{D^+_{tag}}$ and $n^{\mu X}_{D^0_{tag}}$ for both cases of the charged and neutral tagged D mesons, respectively. Figure 7.1 shows the likelihood values L as a function of decay branching fraction $BF(D^+ \to \mu^+ X)$. The maximum of the L_{max} occurs at the branching fraction of $BF(D^+ \to \mu^+ X)$= 17.28% .Figure 7.2 shows the likelihood values L as a function of decay branching fraction $BF(D^0 \to \mu^+ X)$. The maximum of the L_{max} occurs at the branching fraction of $BF(D^0 \to \mu^+ X)$=8.12%.

By integrating both likelihood functions from two sides of the peak position to $\pm\sigma$ value corresponding to 68.3% of the total area below and above the peak position, the statistical errors are obtained. Finally we obtain

$$BF(D^+ \to \mu^+ X) = (17.28^{+6.13}_{-6.13})$$

and

$$BF(D^0 \to \mu^+ X) = (8.12^{+2.09}_{-2.09})\%,$$

where the errors are statistical.

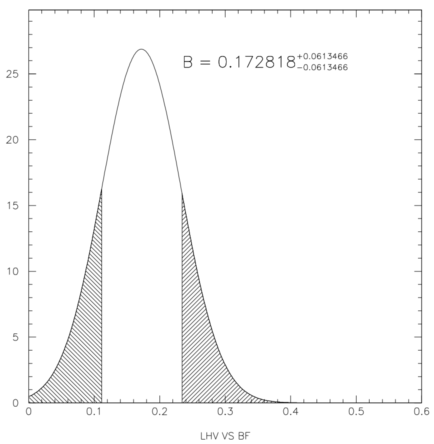

Fig 7.1 Likelihood as a function of the inclusive μ decay branching fraction of charged D

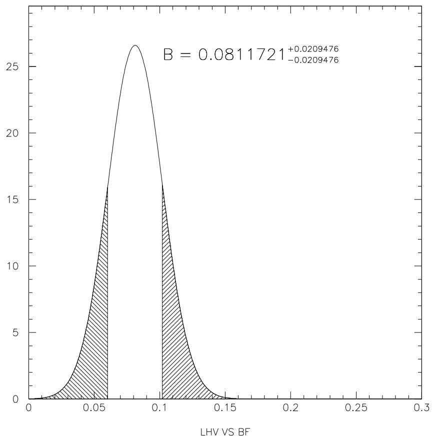

Fig 7.2 Likelihood as a function of the inclusive μ decay branching fraction of neutral D

7.3 Systematic error analysis

Three independent sources of systematic errors have been considered: uncertainties in the numbers of single tagged neutral and charged D mesons due to statistics, uncertainties of ξ and β which are due to uncertainties in values of the production cross section measured and uncertainties in the particle identification efficiencies and particle misidentification rates.

The uncertainties in the numbers of singly tagged neutral and charged D mesons due to statistics is considered to be the number of fluctuations in backgrounds. As a result , we obtain δN_{d0}=40 while δN_{d+}=24. The uncertainties of ξ and β which are due to uncertainties in values of the production cross section measured have been discussed in Ref[2]. We just quoted the results as $\delta\xi$=0.0175, $\delta\beta$=0.0622. The uncertainties in the particle identification efficiencies and particle misidentification rates may also cause an uncertainty in $N^{\mu}_{D^+}$ and $N^{\mu}_{D^0}$. The main part of the uncertainties come from $\pi \to \mu$ misidentification. Using the values of $\delta\eta^{\pi-\mu}$ in table 4.2 and N^{π} in table 5.5-5.8 we get $\delta N^{\mu}_{D^+}$=0.93 and $\delta N^{\mu}_{D^0}$=2.04.

Table 1: Summary on systematic uncertainties in $BF(D^+ \to \mu X)$ and $BF(D^0 \to \mu X)$

Systematic Sources	Uncertainties in $BF(D^0 \to \mu X)$ [%]	Uncertainties in $BF(D^+ \to \mu X)$ [%]
Single Tag	$^{+0.14}_{-0.14}$	$^{+0.44}_{-0.44}$
Number of $\delta N^{\mu}_{D_{tag}}$ caused by uncertainties in η^{a-b}	$^{+0.40}_{-0.40}$	$^{+0.94}_{-0.94}$
ξ and β	$^{+0.44}_{-0.44}$	$^{+1.72}_{-1.72}$
Total	$^{+0.61}_{-0.61}$	$^{+2.01}_{-2.01}$

The systematic uncertainties are summarized in Table 3 in terms of absolute errors on the BF. The combined effect of these sources is obtained by adding in the uncertainties in quadrature, which yields a total systematic error of $^{+0.61}_{-0.61}$% and $^{+2.01}_{-2.01}$% for the D^0 and D^+, respectively. For the systematic error estimating, the uncertainty in luminosity is also taken into account (in η and β). But some uncertainties in Monte Carlo efficiency due to TOF, dE/dx, tracking efficiency, pion and kaon selection cuts have not been considered yet. Quoting both statistical and systematic errors, the decay branching fraction are:

$$BF(D^+ \to \mu^+ X) = (17.28^{+6.13+2.01}_{-6.13-2.01})\%$$

and

$$BF(D^0 \to \mu^+ X) = (8.12^{+2.09+0.61}_{-2.09-0.61})\%.$$

8 Summary

In summary, using a "method of combining the D^+ and D^0 single and 'double'tag together", the inclusive semi-muonic decay branching fractions of the two mesons have been measured. The measured value of the inclusive decay branching fraction of $D^0 \to \mu^+ X$ is consistent with the PDG values.

We first give measured value of the inclusive semi-muonic decay branching fractions of the D^+ mesons, which is not available in PDG booklet at present.

References

[1] G. Rong "Some Ideas to Measure Inclusive Particle 'P' Decay Branching Fractions of D^+ and D^0 Mesons with Data Taken at $\sqrt{s} = 4.03\ GeV$", November 1995.
G. Rong, W.G. Yan, H.W. Zhao, C.C. Xu and C.H. Luo "A Preliminary Result of Measurement of the Inclusive K^{*0}, K^0 Decay Branching Fractions of D^+ and D^0 Mesons", BES Monthly Meeting, IHEP, Beijing, 14 Dec., 1995.

[2] G. Rong, C.H. Luo, W.G. Yan " Measurement of Inclusive ϕ Decay Branching Fractions of $D^{\pm}(D^0)$ Mesons and Search for $D^{\pm} \to \phi e^{\pm} \nu$", 5 August, 1996